

CONJUGATE HEAT TRANSFER ANALYSIS OF A  
BATTERY PACK USING FINITE VOLUME METHOD

BY

IMRAN MOKASHI

A thesis submitted in fulfillment of the requirement for the  
degree of Doctor of Philosophy (Engineering)

Kulliyyah of Engineering  
International Islamic University Malaysia

JANUARY 2022

## ABSTRACT

Lithium-ion (Li-ion) batteries are an excellent energy source for electric vehicles due to their extraordinary features, such as lower mass density, high energy density and long service life. The use of Li-ion batteries in electric vehicles is becoming extensive in the modern world. During battery charging and usage, internal heat is continuously generated due to increased thermal resistance. If the heat produced is not removed correctly, it will get stored and increase the cell temperature. Such an extreme temperature directly affects the life cycle, effectiveness, dependability, and battery safety problems. Hence cooling mechanism is necessary to have a good life and reliability on the battery system. The main objective of this analysis is to perform the thermal analysis of the Li-ion battery pack considering conjugate conduction-convection boundary conditions at the pack and coolant interface. This analysis is performed numerically by solving the relevant governing equations using the finite volume method. The conduction, Navier-Stokes, and energy equations are solved iteratively. The numerical study is carried for the battery pack cooled with five categories of coolants. Five categories of coolants are passed over the heat-generating battery packs to extract the heat and keep the temperature within the limit. Different kinds of gases, conventional oils, thermal oils, nanofluids, and liquid metals, are adopted as coolants. In each category of coolant, five types of fluids are selected to obtain the lowest maximum temperature. The flow Reynolds number ( $Re$ ), heat generation ( $Q_{gen}$ ), and conductivity ratio ( $Cr$ ) are the parameters considered for each fluid to analyze the temperature distribution in the battery pack and its maximum temperature in detail. The average Nusselt number ( $Nu_{avg}$ ) analysis indicates the heat removal from the battery pack cooled by flowing fluid is carried out considering coupled heat transfer conditions at the pack and coolant interface. The  $Pr$  of the coolants varies in the range of 0.0208 to 511.5 (25 coolants), and  $Cr$  for each coolant category has its own upper and lower limit are used. The major findings of the conjugate analysis conducted reveals that the temperature distribution is non-uniform at the top and bottom of the battery. The maximum temperature of the battery pack is located at the top portion of the battery where the electrodes are placed. The temperature of the pack is low at the bottom surface due to direct contact with the coolant which comes in contact as fresh. The regions with high and low temperatures at the top and bottom of the battery pack produce uneven thermal stress, which later can cause the failure of the battery. Hence, choosing an appropriate range of thermal conductivity ratios that balances the solid and the fluid field to get better battery system performance results is required. The maximum temperature of the pack is significantly reduced by the  $Re$  and  $Cr$  of the coolants. While  $Q_{gen}$  in the battery causes an increase in temperature above critical limits. For temperature reduction below the critical threshold requires use of nanofluids at moderate  $Re$  and any  $Cr$  is suitable. The flow of gas coolants over the battery pack causes a less decrease in maximum temperature due to their lower thermal conductivity. The  $Cr$  of all coolants except gases causes a higher difference in maximum temperature at all  $Re$ . Thermal oils, nanofluids, and liquid metals provide maximum temperature in the same range of 0.62 to 0.54. In contrast, gases have nearly the same effect at different values of  $Re$  and  $Cr$ .  $Pr$  of oils and liquid metals show more influence than the gases and nanofluids. However, the  $Pr$  of coolants shows lower effects at different heat generations inside the battery pack. Conversely, by increasing the  $Cr$  of coolants, the  $Pr$  shows a promising variation in maximum temperature. The  $Nu_{avg}$  is found to be unaffected by  $Q_{gen}$  due to the velocity profile remaining the same at any heat generation

term. Whereas the flow  $Re$  changes the velocity distribution significantly which impacts  $Nu_{avg}$  severely for different coolants. The analysis also revealed that  $Cr$  and  $Q_{gen}$  have no role in improving  $Nu_{avg}$  while  $Pr$  and  $Re$  vary significantly in each step. Moreover,  $Nu_{avg}$  is found to increase with  $Re$  continuously irrespective of any  $Cr$  and  $Q_{gen}$ . While, for oils with an increase in  $Pr$  and  $Re$ ,  $Nu_{avg}$  was found to reduce significantly. Nanofluids are found to be more effective in improving heat transfer from the battery pack when cooled by flowing nano-coolants over it.




## ملخص البحث

أصبحت السيارات الكهربائية التي تستخدم نظام بطارية الليثيوم أيون Li-ion واسعة النطاق في العالم الحديث. يمكن اعتبار بطاريات الليثيوم أيون (Li-ion) مصدرًا ممتازًا للطاقة للسيارات الكهربائية نظرًا لخصائصها غير العادية ، مثل كثافة الكتلة المنخفضة ، وكثافة الطاقة العالية ، وعمر الخدمة الطويل ، وما إلى ذلك ، ومع ذلك ، أثناء شحن البطارية واستخدامها ، داخليًا تتولد الحرارة بشكل مستمر بسبب زيادة المقاومة الحرارية. إذا لم تتم إزالة الحرارة الناتجة بشكل صحيح ، فسيتم تخزينها وزيادة درجة حرارة الخلية. تؤثر درجة الحرارة القصوى هذه بشكل مباشر على دورة الحياة والفعالية والاعتمادية ومشاكل سلامة البطارية. ومن ثم فإن آلية التبريد ضرورية للحصول على عمر جيد وموثوقية لنظام البطارية. الهدف الرئيسي من هذا البحث هو إجراء التحليل الحراري لحزمة بطارية Li-ion مع مراعاة ظروف حدود التوصيل والحمل المتقارن في واجهة العبوة والمبرد. يتم إجراء هذا التحليل عدديًا عن طريق حل المعادلات الحاكمة ذات الصلة باستخدام طريقة الحجم المحدد. يتم حل معادلات التوصيل و Navier-Stokes والطاقة بشكل تكراري. يتم إجراء الدراسة العددية لحزمة البطارية المبردة بخمس فئات من المبردات. يتم تمرير خمس فئات من المبردات فوق حزم البطاريات المولدة للحرارة لاستخراج الحرارة والحفاظ على درجة الحرارة ضمن الحد المسموح به. يتم اعتماد أنواع مختلفة من الغازات والزيوت التقليدية والزيوت الحرارية والسوائل النانوية والمعادن السائلة كمبردات. في كل فئة من سائل التبريد ، يتم اختيار خمسة أنواع من السوائل للحصول على أدنى درجة حرارة قصوى. يعتبر رقم رينولدز للتدفق (Re) ، وتوليد الحرارة

( $Q_{gen}$ ) ، ونسبة التوصيل ( $Cr$ ) هي المعلمات التي تم أخذها في الاعتبار لكل مائع لتحليل توزيع درجة الحرارة في حزمة البطارية ودرجة الحرارة القصوى بالتفصيل. علاوة على ذلك ، يشير تحليل متوسط رقم  $Nusselt$  ( $Nu_{avg}$ ) إلى أن إزالة الحرارة من حزمة البطارية المبردة عن طريق السائل المتدفق يتم إجراؤها مع الأخذ في الاعتبار حالة نقل الحرارة المقترنة في العبوة وواجهة المبرد. يتفاوت معدل  $Pr$  للمبردات في النطاق من 0.0208 إلى 511.5 (25 مبردًا) ، ويتم استخدام  $Cr$  لكل فئة من فئات المبرد للحد الأعلى والأدنى الخاص بها. وجد أن درجة الحرارة القصوى تزيد لزيادة  $Q_{gen}$  وتتنخفض لزيادة  $Re$  و  $Cr$ . كما وجد أن الزيوت الحرارية والسوائل النانوية والمعادن السائلة توفر درجة حرارة قصوى في نفس النطاق من 0.62 إلى 0.54. في المقابل ، الغازات لها نفس التأثير تقريبًا عند قيم مختلفة من  $Re$  و  $Cr$ . كشف التحليل أن  $Cr$  و  $Q_{gen}$  ليس لهما دور في تحسين  $Nu_{avg}$  بينما تختلف  $Pr$  و  $Re$  اختلافًا كبيرًا في كل خطوة. علاوة على ذلك ، وجد أن  $Nu_{avg}$  يزداد مع  $Re$  بشكل مستمر بغض النظر عن أي  $Cr$  و  $Q_{gen}$ . بينما ، بالنسبة للزيوت التي تحتوي على زيادة في  $Pr$  و  $Re$  ، وجد أن  $Nu_{avg}$  ينخفض بشكل ملحوظ. كما وجد أن الموائع النانوية تكون أكثر فعالية في تحسين نقل الحرارة من حزمة البطارية عند تبريدها عن طريق تدفق المبردات النانوية فوقها.

## APPROVAL PAGE

The thesis of Imran Mokashi has been approved by the following:



---

Sher Afghan Khan  
Supervisor



---

Muhammad Hanafi Bin Azami  
Co-supervisor



---

Nur Azam Abdullah  
Co-supervisor



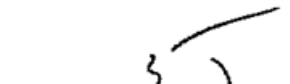
---

Ahmad Faris Ismail  
Internal Examiner



---

Mohd Zulkifly Bin Abdullah  
External Examiner




---

Akram Zeki Khedher  
Chairman

## DECLARATION

I hereby declare that this thesis is the result of my own investigations, except where otherwise stated. I also declare that it has not been previously or concurrently submitted as a whole for any other degrees at IIUM or other institutions.

Imran Mokashi

Signature.......... Date..... 20/01/2022.....



**INTERNATIONAL ISLAMIC UNIVERSITY MALAYSIA**

**DECLARATION OF COPYRIGHT AND AFFIRMATION OF  
FAIR USE OF UNPUBLISHED RESEARCH**

**CONJUGATE HEAT TRANSFER ANALYSIS OF A BATTERY  
PACK USING FINITE VOLUME METHOD**

I declare that the copyright holder of this thesis are jointly owned by the student and IIUM.

Copyright © 2022 Imran Mokashi and International Islamic University Malaysia. All rights reserved.

No part of this unpublished research may be reproduced, stored in a retrieval system, or transmitted, in any form or by any means, electronic, mechanical, photocopying, recording or otherwise without prior written permission of the copyright holder except as provided below

1. Any material contained in or derived from this unpublished research may only be used by others in their writing with due acknowledgement.
2. IIUM or its library will have the right to make and transmit copies (print or electronic) for institutional and academic purpose.
3. The IIUM library will have the right to make, store in a retrieval system and supply copies of this unpublished research if requested by other universities and research libraries.

By signing this form, I acknowledged that I have read and understand the IIUM Intellectual Property Right and Commercialization policy.

Affirmed by Imran Mokashi



.....

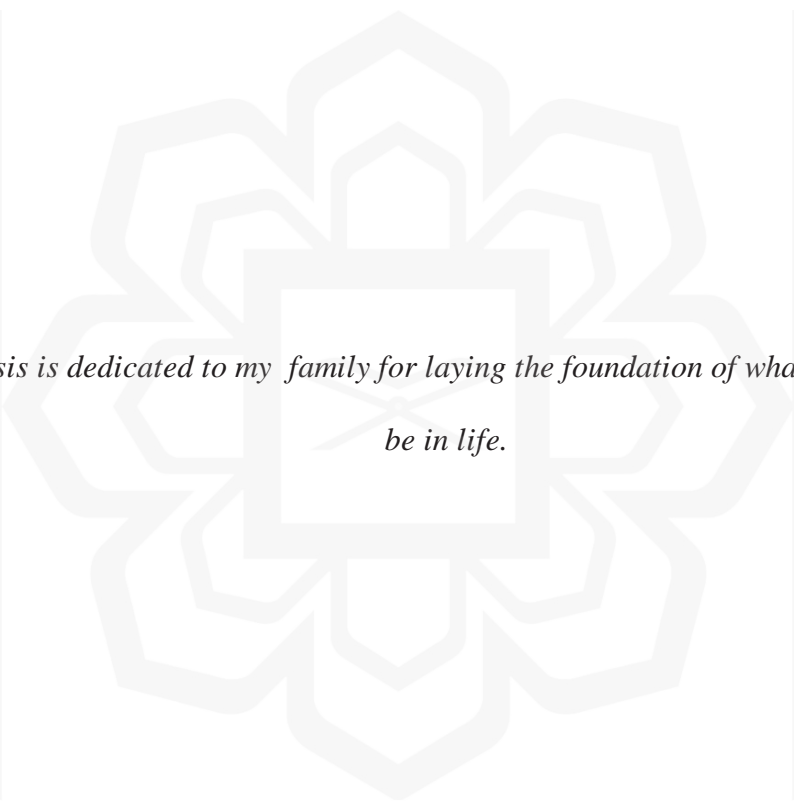
Signature

20/01/2022

.....

Date





*This thesis is dedicated to my family for laying the foundation of what I turned out to  
be in life.*

## ACKNOWLEDGEMENTS

Allah - beginning with the name of - the Most Gracious, the Most Merciful Most Auspicious is he whose control is the entire kingship; and he can do all things [67:1]. All Praise to Allah, the Lord of the creation, and countless blessings and peace upon our Master Mohammed, the leader of the Prophets.

A special thanks to Professor Dr. Sher Afghan Khan for his continuous support, encouragement, and leadership, and for that, I will be forever grateful. He was always there to solve any problem that came to my research. Heartiest thanks to my co-supervisors, Assistant Professor Dr. Muhammad Hanafi Bin Azami, and Assistant Professor Dr. Nur Azam Abdullah, for guidance and support in my research work. I want to thank them for their helpful and inspiring advice as doctoral supervisors and for providing me with the academic freedom to develop and realize new ideas and methods. Their in-depth knowledge has been very beneficial to this research.

It is a great pleasure to express my sincere thanks and gratitude to my fellow friends in the “ECTRMG post-graduate lab” for their friendly cooperation and support.

Special thanks to my dear father Late. Mr. Jalaluddin Mokashi, and mother, Mrs. Khatija Mokashi, Meenaz Mokashi, my wife, sister Sanakousar Shaikh and my beloved daughter Maryam and son Zaki for their prayers, support, encouragement, patience, and appreciation throughout my life. I hope this study somehow acknowledges their effort and determination in confronting all the hardships they have faced while bringing me to this level. Also, I would like to express my sincere appreciation to my visionary Grandfather Late. Mr. Babasaheb Mokashi, and my entire family for the precious support during my tough times before completing this thesis.

Once again, we glorify Allah for His endless mercy on us one of which is enabling us to successfully round off the efforts of writing this thesis. Alhamdulillah

# TABLE OF CONTENTS

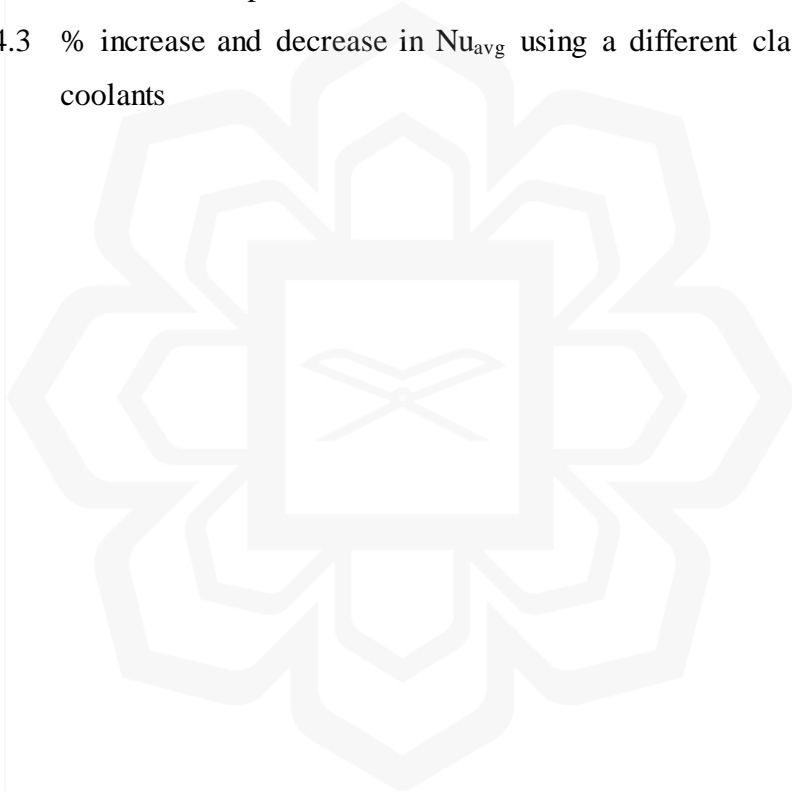
Abstract.....	i
Abstract in Arabic.....	iii
Approval Page.....	v
Declaration.....	vi
Copyright.....	vii
Dedication.....	viii
Acknowledgments.....	ix
List of Tables.....	xii
List of Figures.....	xiii
List of Symbols.....	xvii
List of Abbreviations.....	xx
<b>CHAPTER ONE: INTRODUCTION.....</b>	<b>1</b>
1.1 Battery Thermal Management System (BTMS).....	1
1.2 Problem Statement and its Significance.....	5
1.3 Research Objectives.....	7
1.4 Research Philosophy.....	7
1.5 Research Methodology.....	8
1.6 Research Scope and Limitation.....	9
1.7 Thesis Outline.....	10
<b>CHAPTER TWO: LITERATURE REVIEW.....</b>	<b>12</b>
2.1 Overview.....	12
2.2 Literature Review.....	12
2.2.1 Analytical and mathematical modelling of BTMS.....	12
2.2.2 Air Cooled BTMS.....	14
2.2.3 PCM (phase change material) based BTMS.....	19
2.2.4 CFD (computational fluid dynamics) based BTMS.....	22
2.2.5 Liquid cooled BTMS.....	25
2.2.6 Conjugate analysis of BTMS.....	26
2.3 Summary.....	28
<b>CHAPTER THREE: NUMERICAL METHODOLOGY.....</b>	<b>29</b>
3.1 Overview.....	29
3.2 Physical Model.....	30
3.3 Approximations and Assumptions.....	33
3.4 Mathematical Model.....	34
3.5 Method of Solution.....	44
3.6 Grid Independence Test.....	46
3.7 Validation of the FVM Code.....	47
3.8 Summary.....	51
<b>CHAPTER FOUR: RESULTS AND DISCUSSION.....</b>	<b>52</b>
4.1 Overview.....	52
4.2 Temperature in Solid Battery Pack.....	52
4.3 Temperature Variation in Battery Cooled by Fluids.....	61
4.4 Maximum Temperature Analysis.....	89

4.5 Average Nusselt Number Analysis.....	116
<b>CHAPTER FIVE: CONCLUSION AND FUTURE RECOMMENDATION....</b>	<b>132</b>
5.1 Overview.....	132
5.2 Conclusion.....	132
5.3 Future Scope.....	135
<b>REFERENCES.....</b>	<b>136</b>
<b>PUBLICATIONS AND CONFERENCES.....</b>	<b>159</b>
<b>APPENDIX I: CODE.....</b>	<b>160</b>



## LIST OF TABLES

Table 3.1	Non-dimensional range of parameters obtained	41
Table 3.2	<i>Pr</i> number of five fluids belonging to each category of coolant	42
Table 3.3	Properties of coolants belonging to each category used in this study	43
Table 4.1	Reduction in maximum temperature in % for different <i>Cr</i> of coolants compared to air <i>Cr</i>	112
Table 4.2	Maximum temperature reduction/increment % for different <i>Pr</i> of coolant in comparison with air coolant	114
Table 4.3	% increase and decrease in $Nu_{avg}$ using a different classes of coolants	130



## LIST OF FIGURES

Figure 1.1	Research flow chart	9
Figure 3.1	Schematic view of the arrangement of battery packs with and without the coolant consideration	32
Figure 3.2	The symmetric battery (prismatic cell) and coolant flow domain considered for computational analysis	34
Figure 3.3	Schematic of boundary conditions on half of battery domain	38
Figure 3.4	Schematic of boundary conditions on half of the fluid (coolant) domain	40
Figure 3.5	Numerical computation method flow chart	45
Figure 3.6	Grid independence test for four grid sizes	47
Figure 3.7	Validation of the present FVM code with Ghia et al. (Ghia et al., 1982) at a) $Re = 100$ b) $Re = 1000$	49
Figure 3.8	Present FVM code validation with results from Jahangeer et al. (Jahangeer et al., 2007) and Ramis and Jilani (Ramis et al., 2008)	49
Figure 3.9	Validation of FVM code with experimental work, air $Pr = 0.7$ , and water $Pr = 6.9$	50
Figure 4.1	Biot number ( $Bi$ ) effect on the temperature of the battery	54
Figure 4.2	$T_{max}$ variation with $Bi$ and $Q_{gen}$	54
Figure 4.3	Effect of $Q_{gen}$ on battery temperate with convection from the surface	57
Figure 4.4	Temperature distribution in battery cell for $Q_{gen} = 0.6$	57
Figure 4.5	Temperature distribution in battery cell for $Q_{gen} = 1.0$	58
Figure 4.6	Temperature distribution in battery cell for $Q_{gen} = 1.5$	58
Figure 4.7	Temperature distribution in battery cell for $Bi = 2$	59
Figure 4.8	Temperature distribution in battery cell for $Bi = 5$	60
Figure 4.9	Temperature distribution in battery cell for $Bi = 15$	60
Figure 4.10	Effect of $Re$ on $T_b$ along axial direction (Air)	62
Figure 4.11	Effect of $Re$ on $T_b$ along axial direction (Water)	62
Figure 4.12	Effect of $Q_{gen}$ on $T_b$ along axial direction (Air)	64
Figure 4.13	Effect of $Q_{gen}$ on $T_b$ along axial direction (Water)	65

Figure 4.14	Effect of $Pr$ on $T_b$ (Gases)	66
Figure 4.15	Effect of $Pr$ on $T_b$ along axial direction (Oils)	67
Figure 4.16	Effect of $Pr$ on $T_b$ along axial direction (Nanofluids)	68
Figure 4.17	Effect of $Pr$ on $T_b$ along axial direction (Liquid metals)	69
Figure 4.18	Effect of $Pr$ on $T_b$ along axial direction (Thermal oils)	70
Figure 4.19	Effect of $Cr$ on $T_b$ along axial direction (Gases)	71
Figure 4.20	Effect of $Cr$ on $T_b$ along axial direction (Oils)	72
Figure 4.21	Effect of $Cr$ on $T_b$ along axial direction (Thermal oils)	73
Figure 4.22	Effect of $Cr$ on $T_b$ along axial direction (Nanofluids)	74
Figure 4.23	Effect of $Cr$ on $T_b$ along axial direction (Liquid metals)	75
Figure 4.24	Effect of $Pr$ on $T_b$ in transverse direction (Nanofluids)	77
Figure 4.25	Effect of $Q_{gen}$ on $T_b$ in transverse direction (Water)	77
Figure 4.26	Effect of $Re$ on $T_b$ in transverse direction (Water)	78
Figure 4.27	Effect of $Cr$ on $T_b$ in transverse direction (Water)	79
Figure 4.28	Temperature contours in battery pack when $Pr = 0.7$ (Air)	81
Figure 4.29	Temperature contours in battery pack when $Pr = 6.9$ (Water)	81
Figure 4.30	Temperature contours in battery pack $Pr = 21.7$ (Dielectric oil)	83
Figure 4.31	Temperature contours in battery pack $Pr = 101.5$ (Syltherm 800)	84
Figure 4.32	Temperature contours in battery pack for $Pr = 0.0303$ (GaIn <sup>20</sup> )	85
Figure 4.33	Temperature contours in battery pack when $Cr = 0.1$ (Water)	85
Figure 4.34	Temperature contours in battery pack when $Cr = 0.5$ (Water)	87
Figure 4.35	Temperature contours in battery pack when $Cr = 1.0$ (Water)	87
Figure 4.36	Temperature contours in battery pack when $Cr = 1.5$ (Water)	88
Figure 4.37	Temperature contours in battery pack when $Cr = 2.0$ (Water)	88

Figure 4.38	$T_{b(max)}$ in battery pack as a function of $Re$ and heat generation ( $Q_{gen}$ ) for air	90
Figure 4.39	$T_{b(max)}$ in battery pack as a function of $Re$ and heat generation ( $Q_{gen}$ ) for water	91
Figure 4.40	$T_{b(max)}$ in battery pack as a function of $Re$ and $Cr$ for various gases ( $Pr$ )	93
Figure 4.41	$T_{b(max)}$ in battery pack as a function of $Re$ and $Cr$ for various Common oils	93
Figure 4.42	$T_{b(max)}$ in battery pack as a function of $Re$ and $Cr$ for various Thermal oils	94
Figure 4.43	$T_{b(max)}$ in battery pack as a function of $Re$ and $Cr$ for various Nanofluids	94
Figure 4.44	$T_{b(max)}$ in battery pack as a function of $Re$ and $Cr$ for various Liquid metals	95
Figure 4.45	$T_{b(max)}$ in battery pack as a function of $Re$ and $Pr$ of Gases	97
Figure 4.46	$T_{b(max)}$ in battery pack as a function of $Re$ and $Pr$ of Common oils	97
Figure 4.47	$T_{b(max)}$ in battery pack as a function of $Re$ and $Pr$ of Thermal oils	98
Figure 4.48	$T_{b(max)}$ in battery pack as a function of $Re$ and $Pr$ of Nanofluids	98
Figure 4.49	$T_{b(max)}$ in battery pack as a function of $Re$ and $Pr$ of Liquid metals	99
Figure 4.50	$T_{b(max)}$ in battery pack as a function of $Cr$ and $Q_{gen}$ for Gases	101
Figure 4.51	$T_{b(max)}$ in battery pack as a function of $Cr$ and $Q_{gen}$ for Common oils	101
Figure 4.52	$T_{b(max)}$ in battery pack as a function of $Cr$ and $Q_{gen}$ for Thermal oils	102
Figure 4.53	$T_{b(max)}$ in battery pack as a function of $Cr$ and $Q_{gen}$ for Nanofluids	102
Figure 4.54	$T_{b(max)}$ in battery pack as a function of $Cr$ and $Q_{gen}$ for Liquid metals	103
Figure 4.55	$T_{b(max)}$ in battery pack varying with $Q_{gen}$ for $Pr$ of Gases	104
Figure 4.56	$T_{b(max)}$ in battery pack varying with $Q_{gen}$ for $Pr$ of Common oils	105
Figure 4.57	$T_{b(max)}$ in battery pack varying with $Q_{gen}$ for $Pr$ of Thermal oils	105

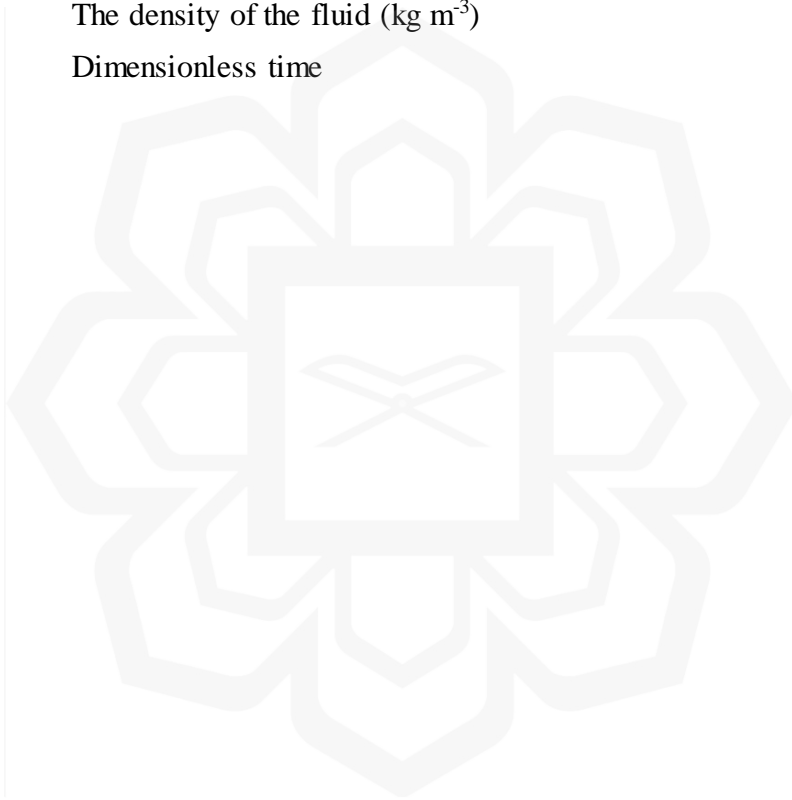


Figure 4.58	$T_{b(max)}$ in battery pack varying with $Q_{gen}$ for $Pr$ of Nanofluids	106
Figure 4.59	$T_{b(max)}$ in battery pack varying with $Q_{gen}$ for $Pr$ of Liquid metals	106
Figure 4.60	$T_{b(max)}$ in battery pack varying with $Cr$ and $Pr$ of Gases	108
Figure 4.61	$T_{b(max)}$ in battery pack varying with $Cr$ and $Pr$ of Common oils	108
Figure 4.62	$T_{b(max)}$ in battery pack varying with $Cr$ and $Pr$ of Thermal oils	109
Figure 4.63	$T_{b(max)}$ in battery pack varying with $Cr$ and $Pr$ of Nanofluids	109
Figure 4.64	$T_{b(max)}$ in battery pack varying with $Cr$ and $Pr$ of Liquid metals	110
Figure 4.65	Average Nusselt number ( $Nu_{avg}$ ) increase with $Re$ for air and water vs. $Q_{gen}$	117
Figure 4.66	$Nu_{avg}$ for different $Re$ with gases and oils as coolants	119
Figure 4.67	$Nu_{avg}$ for different $Re$ with thermal oils, nanofluids, and liquid metals as coolant	120
Figure 4.68	$Nu_{avg}$ for different $Re$ and $Cr$ belonging to five classes of coolants	121
Figure 4.69	No effect of $Q_{gen}$ term on $Nu_{avg}$ whereas oils and nanofluids maximum $Nu_{avg}$	122
Figure 4.70	$Nu_{avg}$ for $Pr$ of gases with increasing heat generation	124
Figure 4.71	$Nu_{avg}$ for $Pr$ of common oils with increasing heat generation	124
Figure 4.72	$Nu_{avg}$ for $Pr$ of thermal oils with increasing heat generation	125
Figure 4.73	$Nu_{avg}$ for $Pr$ of nanofluids with increasing heat generation	125
Figure 4.74	$Nu_{avg}$ for $Pr$ of liquid metals with increasing heat generation	126
Figure 4.75	$Nu_{avg}$ for different $Pr$ of gases with increasing conductivity ratio	127
Figure 4.76	$Nu_{avg}$ for different $Pr$ of oils with increasing conductivity ratio	128
Figure 4.77	$Nu_{avg}$ for different $Pr$ of thermal oils with increasing conductivity ratio	128
Figure 4.78	$Nu_{avg}$ for different $Pr$ of nanofluids with increasing conductivity ratio	129
Figure 4.79	$Nu_{avg}$ for different $Pr$ of liquid metals with increasing conductivity ratio	129

## LIST OF SYMBOLS

$Ar$	Aspect ratio
$Bi$	Biot number
$C$	Specific heat ( $\text{Jkg}^{-1}\text{K}^{-1}$ )
$Cr$	Conductivity ratio
$H$	Battery height (mm)
$h$	Convective heat transfer coefficient ( $\text{Wm}^{-2}\text{K}^{-1}$ )
$k$	Thermal conductivity ( $\text{Wm}^{-1}\text{K}^{-1}$ )
$k_b$	Thermal conductivity of battery material ( $\text{Wm}^{-1}\text{K}^{-1}$ )
$k_f$	Thermal conductivity of the fluid ( $\text{Wm}^{-1}\text{K}^{-1}$ )
$k_s$	Thermal conductivity of solid (battery) ( $\text{Wm}^{-1}\text{K}^{-1}$ )
$L$	Battery length (mm)
$Nu$	Nusselt number
$Nu_{avg}$	Average nusselt number
$Nu_x$	Local nusselt number
$P$	Dimensionless pressure
$p$	Pressure
$p'$	Corrected pressure (Pa, $\text{Nm}^{-2}$ )
$Pr$	Prandtl number
$Q_{gen}$	Dimensionless volumetric heat generation
$q'''$	Volumetric heat generation ( $\text{Wm}^{-3}$ )
$Re$	Reynolds number
$T$	Non-dimensional temperature
$t$	Time (s, min)
$T^*$	Temperature ( $^{\circ}\text{C}$ , K)
$T_{\infty}$	Surrounding temperature ( $^{\circ}\text{C}$ , K)
$T_{bmax}$	Battery maximum temperature ( $^{\circ}\text{C}$ , K)
$T_{max}$	Maximum temperature ( $^{\circ}\text{C}$ , K)
$T_o$	Initial temperature ( $^{\circ}\text{C}$ , K)
$U$	Dimensionless velocity along the axial direction
$u^*$	Velocity long the axial direction ( $\text{ms}^{-1}$ )
$u_{\infty}$	Free stream velocity ( $\text{ms}^{-1}$ )
$V$	Dimensionless velocity along the transverse direction
$v^*$	Velocity along the transverse direction ( $\text{ms}^{-1}$ )

$w_b$	Half Battery width (mm)
$w_f$	Half spacing between two parallel battery cells (mm)
$w_s$	Half battery width (mm)
$x$	Battery axial length (mm)
$X$	Dimensionless battery length
$y_s$	Battery width (mm)
$Y_s$	Dimensionless battery width
$\alpha$	Thermal diffusivity of fluid ( $\text{m}^2\text{s}^{-1}$ )
$\mu$	Dynamic viscosity ( $\text{Nms}^{-1}$ )
$\nu$	Kinematic viscosity of the fluid ( $\text{m}^2\text{s}^{-1}$ )
$\rho$	The density of the fluid ( $\text{kg m}^{-3}$ )
$\tau$	Dimensionless time



## LIST OF ABBREVIATIONS

1-D	One dimensional
2-D	Two dimensional
3-D	Three dimensional
Al <sub>2</sub> O <sub>3</sub>	Aluminum oxide
BCSs	Battery Cooling Systems
BTMS	Battery Thermal Management System
CFD	Computational Fluid Dynamics
CuO	Copper oxide
DoD	Depth of Discharge
EG	Ethylene Glycol
EVs	Electric Vehicles
FEM	Finite Element Method
FVM	Finite Volume Method
Ga	Gallium
GaIn	Gallium Indium
GaInSn	Gallium Indium Tin, Galinstan brand eutectic alloy
HEV	Hybrid Electric Vehicle
Li Co O <sub>2</sub>	Lithium Cobalt Oxygen
LiB	Lithium-ion Battery
LIBs	Lithium Ion Batteries
Li-ion	Lithium ion
MWCNT	Multi-walled carbon nanotubes
NaK	Sodium Potassium
NCM	Nickel Cobalt Manganese battery
PCM	Phase Change Material
SIMPLE	Semi IMPLICIT Pressure Linked Equation
SOR	Successive over-relaxation
TiO <sub>2</sub>	Titanium dioxide
viz	That is, namely

# CHAPTER ONE

## INTRODUCTION

### 1.1 BATTERY THERMAL MANAGEMENT SYSTEM (BTMS)

The use of Li-ion batteries facilitates power for transmission in electric vehicles. But they are susceptible to heat generation during charging and discharging (An et al., 2017)(Yun et al., 2016). The batteries operating under high-temperature and low-temperature environments require enhanced electrochemical stability to prevent overheating. A BTM system with battery packs must be mounted to improve temperature uniformity and ensure that the battery works within the optimal temperature range (Hannan et al., 2017).

BTMS is classified in a wide range of parameters. The operating principle or the coolant phase and whether or not there is a direct interaction between the coolant and the batteries. The operation is actively controlled by a control system or passively without a power-assisted control system. The BTMS can also be classified based on the coolant phase. The most widely used and suggested coolants in the literature are gas, liquid, and phase change material (Lazrak et al., 2018).

Air-based cooling systems are the most commonly used cooling systems in everyday life, be it for automotive applications, device cooling, or residential applications (Choi et al., 2012; Choi & Kang, 2014; Fan et al., 2013; Fathabadi, 2014; Park, 2013b). Air BCSs use cold air flow between the batteries inside the battery pack to assimilate the produced heat and transfer it away from the batteries. For air BCSs (battery cooling systems), the air flow may be either due to the vehicle's movement, which is alluded to as natural air-driven BCS, or air is forced between the batteries through a power-assisted system.

The majority of the airflow BTMS proposed for EVs (electric vehicles) are forced convection air cooling systems. These systems have a high heat transfer coefficient, low price, simple design, and easy maintenance. The energy consumption during the operation of these devices is low due to lower air viscosity. The air-based

BTMSs proposed in the literature are suggested primarily for battery packs subjected to moderate refrigeration loads.

The battery pack's layout structure, such as the spacing between batteries, array configuration, airflow rate, geometries of inlet and outlet flow ducts, and so on, has a significant impact on BTM system efficiency (Fan et al., 2013; Marambio et al., 2016; Tong et al., 2016; Wang et al., 2014; Yang et al., 2015). Irregular spacing dramatically affects the temperature distribution in the battery cells (Fan et al., 2013). Battery array configuration includes two typical cell arrangements, staggered and aligned. The staggered arrangement of battery cells gives lower maximum temperature in the battery cells than aligned (Tong et al., 2016). Transverse gaps and longitudinal gaps should also be considered for different battery arrangements (Yang et al., 2015). Air flow rate is another crucial parameter that directly affects the efficiency of an air BTMS (Choi & Kang, 2014; Giuliano et al., 2012; Li et al., 2013; Saw et al., 2016; Wang et al., 2015; Xun et al., 2013). When the air flow rate decreases, the maximum temperature of the battery and maximum temperature difference within the battery cells increases. Although the rise in air flow rate would undoubtedly boost the cooling potential for air cooling systems, it also raises the cost. Therefore, consideration should be given to the trade-offs among these two parameters (Tong et al., 2016).

The geometry of Inlet and outlet flow channels plays a significant role in maintaining uniformity in the flow rates across the channels. That, in turn, substantially affects the battery cell temperature and battery module pressure drop (Sun & Dixon, 2014). Two types of air ducts- standard channel and jet cooling channel are reported in the literature. The Jet air cooling significantly reduces the maximum temperature in the battery cells and increases the temperature uniformity within the battery cells. The inclusion of aluminum porous metal foam in an air-cooled BTMS with flow channels also improves the thermal performance of the battery (Mohammadian & Mousavi, 2015).

To date, liquid-based cooling systems have become the most commonly used and popular BTMS, with some of the key producers of EV and HEV (hybrid electric vehicles) using liquid cooling systems to keep the batteries within the safe limit. Rimac Automobili in Croatia produced the first high-performance EVs, which introduced the

liquid-based cooling system to keep the temperature of the batteries at optimal operating conditions. The air-based cooling system appears to be inadequate to keep the battery temperature within the allowable limit at higher ambient temperature. It is more apparent for the high discharge rate of a large battery pack.

Liquid-based BCSs are power-assisted devices that use liquid-phase coolants (Richard, 1999). The liquid coolant passes between the batteries and absorbs some or all of the battery's heat. Liquid-based systems allow auxiliary devices to recycle the liquid coolant by extracting the absorbed heat from the battery pack, unlike air-based BCSs. Liquid cooling, which uses convection or boiling mode to transfer the heat, effectively reduces the temperature and prevents overheating of batteries than air cooling due to the higher specific heat of liquids. Although it has some disadvantages, as stated in (Pesaran 2001)(Chen et al., 2016), liquid cooling is more efficient than air cooling.

The liquid cooling system can be classified into two types as direct-contact and indirect-contact type, depending on whether the working fluid touches the battery directly or not. The most commonly used working fluid for direct-contact type can be dielectric, such as mineral oils (Karimi & Li, 2013; Nelson et al., 2002), electronic cooling liquid (Gils et al., 2014; Hirano et al., 2014), and so on, to prevent short-circuit if the coolant touches the battery directly. The indirect-contact type uses a cold plate or heat sink, jacket, and tubes (pipes) to isolate the battery and the working fluid. Battery-generated heat is conducted from the battery cells into the cooling plate and convected away by the coolant. The selection range for the coolant is broad due to no restriction on the insulation criteria. However, the seal is critical to prevent liquid leakage because the insulation of the working fluid is not taken into account. Further, the working fluid chosen should have low maintenance problems to prevent the shift of the liquid-solid phase under lower ambient temperature, affecting the cooling system and the battery modules due to volume expansion.

Cooling plate (indirect type) has attracted much attention of researchers in BTMS due to smaller thickness, compact structure, and good heat transfer impacts (Giuliano et al., 2012; Huo et al., 2015; Nieto et al., 2014; Panchal et al., 2016a, 2016c, 2016b; Qian et al., 2016; Smith et al., 2014; Tong et al., 2015). Generally, the cold plate

arrangement involves sandwiching batteries within the cooling plates or positioning the cooling plates on the bottom or side surface of the battery. The average increase in temperature and non-uniformity of temperature decreases with the number of batteries between the cooling plates (Tong et al., 2015). While the increase in the volume of the fluid or increase in thickness of the cooling plate decreases the average temperature considerably and increases battery cell uniformity, it also causes an increase in the pumping power. BTMS system design should comprehensively consider electrochemical and thermal-hydraulic parameters. In order to optimize the different parameters, a multi-objective optimization algorithm can be proposed to achieve optimal decisions and acceptable compromises among these parameters. A simple U-flow is the best compromise between thermal efficiency, power consumption, and vehicle integration (Smith et al., 2016).

The cooling plate's operating characteristics are determined in part by the channel's geometric structure: its direction, width, length, etc. It is known that heat transfer by convection decreases along the axial direction of a traditional straight channel due to the development of a hydrodynamic boundary layer resulting in a substantial temperature gradient on the battery surface. Hence to boost efficiency, traditional straight channels are replaced by oblique mini channels. In oblique mini channels, re-initialization of boundary layers takes place, which considerably improves the temperature uniformity of the battery system.

Tubes (pipes) have recently emerged as a valuable constituent of liquid cooling systems (Lan et al., 2016; Rao et al., 2016). U-shape pipe, along with an optimum combination of velocity and other parameters, significantly reduces the temperature uniformity in the channels.

The various cooling specifications for the BTMS system are also determined by the shape and atmosphere of the batteries. In the cylindrical battery, due to the cambered exterior surface, it is not ideal for cooling the battery using a flat cooling plate. The cooling plate structure should be altered and optimized to increase the contact surface between the battery and cooling plate and enhance the cooling effect. The direction of flow, number of channels, and inlet size, and flow rate all affect the BTMS performance.